RSC Advances

PAPER

Cite this: *RSC Adv.*, 2024, **14**, 3798

Supramolecular nanoarchitectonics of propionylated polyrotaxanes with bulky nitrobenzyl stoppers for light-triggered drug release†

Shunyao Zhang, Atsushi Tamura * and Nobuhiko Yui

Cyclodextrin (CD)-based polyrotaxanes (PRXs) are supramolecular polymers comprising multiple CDs mechanically interlocked onto a linear polymer chain by capping the polymer ends with bulky stoppers. Among various PRX derivatives, propionylated PRXs (Pr-PRXs) composed of propionylated α-CD and high molecular-weight poly(ethylene glycol) (PEG) form self-assembled nanoparticles in aqueous solution through hydrophobic interactions. Although Pr-PRX nanoparticles can encapsulate hydrophobic drugs in their hydrophobic domains, their release rate is limited. To improve the efficiency of drug release from Pr-PRX nanoparticles, ultraviolet (UV) light-dissociable Pr-PRXs were designed using 4,5-dimethoxy 2-nitrobenzyl groups as UV-cleavable bulky stopper molecules to facilitate UV-induced drug release. Photodegradable Pr-PRX (Pr-PD-PRX) was synthesized, and its UV-induced dissociation was examined. Pr-PD-PRX was completely dissociated *via* UV irradiation (365 nm) for 30 min. Additionally, Pr-PD-PRX nanoparticles encapsulating hydrophobic drugs collapsed upon UV irradiation, which promoted the release of the encapsulated drugs compared to non-degradable Pr-PRX nanoparticles. UV irradiation of drug-loaded Pr-PD-PRX nanoparticles resulted in higher cytotoxicity than non-irradiated Pr-PD-PRX and non-degradable Pr-PRX. Consequently, designing photodegradable PRX-based nanoparticles provides new insights into developing photoresponsive drug carriers and smart biomedical materials.

Received 9th January 2024
Accepted 18th January 2024

DOI: 10.1039/d4ra00213j

rsc.li/rsc-advances

1. Introduction

Polyrotaxanes (PRXs) are representative interlocked polymers, in which multiple cyclic molecules are mechanically interlocked on a linear polymer axis by capping the polymer terminal ends with bulky stoppers.[1,2] Especially, PRXs composed of α-cyclodextrin (α-CD) as the cyclic molecule and poly(ethylene glycol) (PEG) as the polymer axis have been extensively studied.[3] Recently, CD-based PRXs have attracted considerable interest in the fields of healthcare, biomaterials, and drug delivery systems,[4–8] because of their unique properties, such as the molecular mobility of threading CDs along the polymer axis and biocompatibility of constituent α-CD and PEG. Additionally, PRXs show a unique stimuli-induced dissociation character when the cleavable linkages are introduced on the polymer axis.[6,7,9,10] PRXs that can dissociate in response to various chemical and physical stimuli, such as reductive molecules, pH, reactive oxygen species, and light, have been developed.[9–18] Such stimuli-dissociable PRXs have been utilized to develop novel biomaterials, such as drug delivery carriers,[11,13] therapeutic candidates for metabolic diseases,[12,19] scaffolds for therapeutic cells,[20] and detachable dental adhesives.[14,15] Therefore, stimuli-dissociable PRXs would contribute to the development of biomaterials with novel functionality.

Our group has reported the chemical properties of acylated PRXs, such as solubility in aqueous media, self-assembly, and temperature-responsivity.[21–25] Interestingly, PRXs composed of acylated α-CD and high molecular-weight PEG (M_n = 100 000) self-assemble into nanoparticles in aqueous solution through the hydrophobic interaction of acyl groups.[21,22] The acylated PRX nanoparticles can encapsulate hydrophobic drugs (*e.g.*, paclitaxel (PTX)) into their hydrophobic domain.[21,22] Modifying propionyl groups on PRXs is optimal for loading large amounts of PTX with good dispersion stability.[22] However, the release rate of PTX is limited, and only 40 to 60% of loaded PTX was released from propionylated PRX (Pr-PRX) nanoparticles.[22] To improve the release rate of loaded drugs from Pr-PRX nanoparticles, we conceived using the above-mentioned stimuli-dissociable PRXs. Among the various physical and chemical stimuli, we focused on light irradiation in this study. In general, the degradation rate of light-responsive polymers can be

Department of Organic Biomaterials, Institute of Biomaterials and Bioengineering, Tokyo Medical and Dental University (TMDU), 2-3-10 Kanda-Surugadai Chiyoda, Tokyo 101-0062, Japan. E-mail: tamura.org@tmd.ac.jp

† Electronic supplementary information (ESI) available. See DOI: https://doi.org/10.1039/d4ra00213j

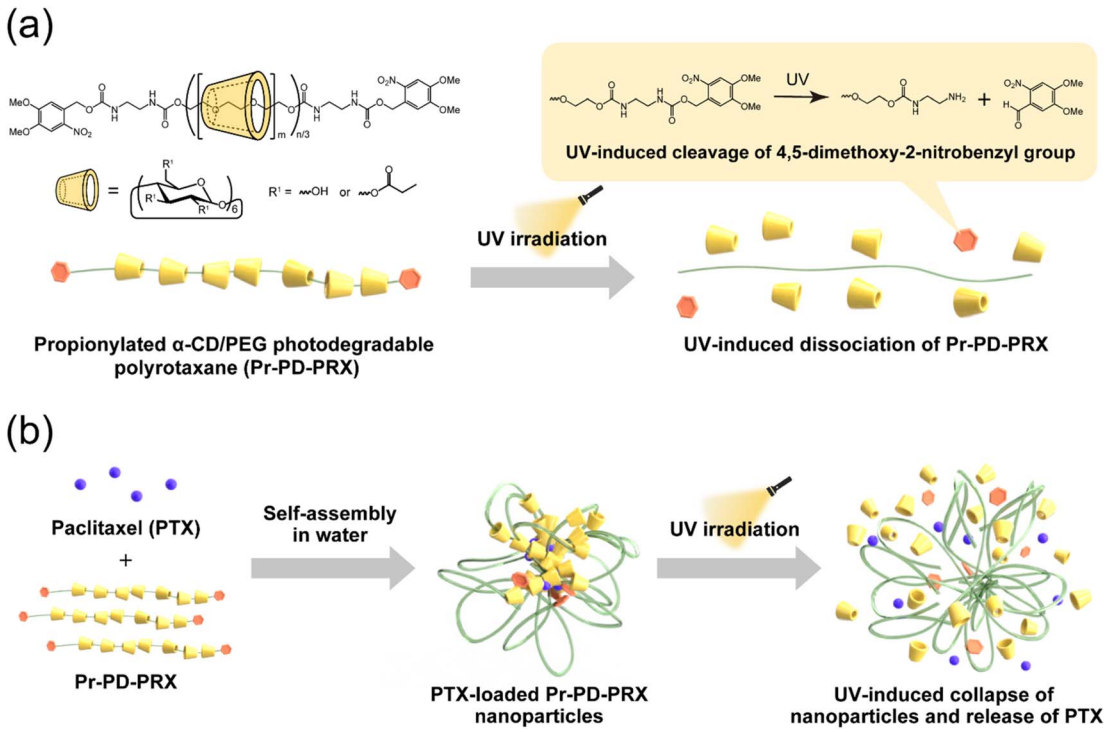

Fig. 1 (a) Schematic illustration of propionylated α-CD/PEG photodegradable polyrotaxanes (Pr-PD-PRXs) and their UV-induced dissociation through the cleavage of 4,5-dimethoxy-2-nitrobenzyl stopper molecules. (b) Formation of paclitaxel (PTX)-loaded Pr-PD-PRX nanoparticles and their UV-induced collapse and subsequent release of PTX.

controlled by adjusting the light wavelength, intensity, and duration of irradiation.[26] On the contrary, other stimuli, such as pH, make it difficult to control the degradation process. Accordingly, we utilized ultraviolet (UV)-cleavable 4,5-dimethoxy-2-nitrobenzyl groups as the stopper for PRXs (Fig. 1a) because this group is sufficiently bulky to interlock threaded α-CDs onto the PEG chain.[17,18] We consider that the UV irradiation of photodegradable Pr-PRX (Pr-PD-PRX) nanoparticles leads to the collapse of the nanoparticles and accelerates the release of loaded drugs (Fig. 1b). Light irradiation-induced release of drugs is achieved using amphiphilic diblock copolymer micelles comprising hydrophilic polymers and hydrophobic polymers containing photocleavable groups in the side chains.[26–30] However, these systems require the cleavage of multiple photocleavable groups to collapse the micelles and release drugs. In contrast, Pr-PD-PRX nanoparticles can more efficiently release drugs than photo-responsive diblock copolymer micelles because Pr-PD-PRX nanoparticles immediately collapse by the cleavage of only a single site of UV-cleavable stoppers.

In this study, UV-dissociable Pr-PD-PRXs capped with bulky 4,5-dimethoxy-2-nitrobenzyl groups were synthesized, and their UV-induced dissociation and self-assembly in aqueous solutions were investigated and compared with those of nondegradable Pr-PRXs (Pr-ND-PRXs) capped with adamantyl groups. UV-induced release and cytotoxicity were examined using the PTX-loaded photodegradable Pr-PD-PRX nanoparticles. The design of the UV-dissociable PRX nanoparticles described herein provide new insights into developing smart light-responsive drug carriers and biomaterials.

2. Experimental

2.1 Materials

PEG (M_n 100 000) was purchased from Merck (Darmstadt, Germany). PEG with terminal amino groups was (PEG-NH_2) synthesized as previously described.[31] α-Cyclodextrin (α-CD) was obtained from Ensuiko Sugar Refining (Tokyo, Japan). Nondegradable PRX (ND-PRX) containing adamantyl groups as stopper molecules was synthesized as previously described.[21] The number of threading α-CDs and the number-average molecular weight of the ND-PRX were 223 and 317 000. 4,5-Dimethoxy-2-nitrobenzyl 4-nitrophenyl carbonate was synthesized as described in ESI.† *N*,*N*-Diisopropylethylamine (DIPEA), propionic anhydride, and paclitaxel (PTX) were obtained from Tokyo Chemical Industry (Tokyo, Japan). *N*,*N*-Dimethyl 4-aminopyridine (DMAP) and lithium chloride (LiCl) were obtained from Fujifilm Wako Pure Chemical (Osaka, Japan). All other reagents and solvents were obtained from Kanto Chemical (Tokyo, Japan) and Fujifilm Wako Pure Chemical.

2.2. Characterization of PRX

^{1}H nuclear magnetic resonance (NMR) spectra were recorded using a Bruker Avance III 400 MHz spectrometer (Bruker BioSpin, Rheinstetten, Germany) in dimethyl sulfoxide (DMSO)-d_6 and NaOD/D_2O at 25 °C. The chemical shifts in ^{1}H NMR spectra

were referenced to DMSO (2.5 ppm in DMSO-d_6) and HDO (4.65 ppm in D_2O). Size exclusion chromatography (SEC) was performed using a Prominence-i LC-2030 Plus system (Shimadzu, Kyoto, Japan) equipped with an RID-20A refractive index (RI) detector and a combination of TSKgel α-4000 and α-2500 columns (300 mm length, 7.8 mm internal diameter; Tosoh, Tokyo, Japan). Sample solutions were injected into the system and eluted with DMSO containing 10 mM LiBr at a flow rate of 0.35 mL min^{-1} at 60 °C. Peaks were detected using the RI and UV absorption at 352 nm.

2.3. Synthesis of photodegradable PRX (PD-PRX)

α-CD (20.0 g, 20.6 mmol) was dissolved in distilled water (125 mL). PEG-NH_2 (4.0 g, 40.0 μmol) dissolved in distilled water (25 mL) was added to this solution, and the mixture was stirred for 24 h at room temperature. The precipitate was collected by centrifugation (7000 rpm) and freeze-dried to obtain pseudopolyrotaxane (21.78 g). Then, 4,5-dimethoxy-2-nitrobenzyl 4-nitrophenyl carbonate (302.5 mg, 800 μmol) and DIPEA (1.39 mL, 800 μmol) were dissolved in dehydrated *N*,*N*-dimethylformamide (DMF; 100 mL). Pseudopolyrotaxane was added to this solution, stirring the mixture for 24 h at room temperature. After the reaction, the precipitate was collected *via* centrifugation (7000 rpm). The precipitate was dissolved in a small aliquot of DMSO, reprecipitated in distilled water, and collected by centrifugation (7000 rpm). The reprecipitation process was repeated until the free α-CD and unreacted reagents were removed. The recovered precipitate was freeze-dried to obtain PD-PRX (5.21 g, 46.9% yield based on recovered PEG mol%). The number of threading α-CDs in the PD-PRX was determined by ^{1}H NMR in NaOD/D_2O comparing the integrated area between 4.84 ppm (H-1 of threaded α-CD in PRX) and 3.21–3.96 ppm (m, –O–CH_2–CH_2– of PEG, H-2, H-3, H-4, H-5, and H-6 protons of α-CD). ^{1}H NMR (400 MHz, NaOD/D_2O) δ = 3.21–3.96 (m, –O–CH_2–CH_2– of PEG, H-2, H-3, H-4, H-5, and H-6 protons of α-CD), 4.84 (m, H-1 proton of α-CD), 7.01 (s, 3-position in 4,5-dimethoxy-2-nitrobenzyl), 7.69 (s, 6-position in 4,5-dimethoxy-2-nitrobenzyl), 8.27 (s, carbamate).

2.4. Synthesis of propionylated PD-PRX (Pr-PD-PRX)

The propionyl groups were modified on PD-PRX as described in a previous study.[22] Briefly, PD-PRX (500 mg, 1.31 μmol PRX, 6.81 mmol hydroxy groups in PRX), propionic anhydrides (2 mol equivalent to hydroxy groups in PRX), and DMAP (50 mg, 409 μmol) were dissolved in 8% LiCl/DMF (25 mL) under a nitrogen atmosphere. The solution was stirred for 24 h at room temperature. The solution was dialyzed against distilled water for 3 days at 4 °C using a Spectra/Por 4 (molecular weight cut-off of 12 000–14 000; Spectrum Laboratories, Rancho Dominguez, CA, USA) and then freeze-dried to obtain Pr-PD-PRX (576.7 mg, 92.9% yield). The propionylated nondegradable PRX (Pr-ND-PRX) was synthesized in the same manner. The number of propionyl groups modified on PD-PRX and ND-PRX was determined by ^{1}H NMR in DMSO-d_6 by comparing the integrated area between 4.72–5.38 ppm (H-1 of threaded α-CD in PRX) and 1.00 ppm (CH_3– of propionyl group). The characteristics of the propionylated PRXs are summarized in Table 1. ^{1}H NMR (400 MHz, DMSO-d_6) δ = 1.00 (CH_3–CH_2–C(=O)– of propionyl group), 2.31 (CH_3–CH_2–C(=O)– of propionyl group), 3.17–4.72 (m, –O–CH_2–CH_2– of PEG, H-2, H-3, H-4, H-5, and H-6 protons of α-CD, OH-6 protons of α-CD), 4.72–5.38 (m, H-1 proton of α-CD), 5.40–6.27 (m, OH-2 and OH-3 protons of α-CD).

2.5. UV-induced degradation of Pr-PD-PRX

Pr-PD-PRX and Pr-ND-PRX were dissolved in DMSO at 10 mg mL^{-1} concentration. The solutions were then exposed to UV light for 1–30 min using a UV light-emitting diode (LED) (MBRL-CUV7530-2, Moritex, Saitama, Japan; emission peak wavelength: 365 nm, power: 7.03 mW cm^{-2}). The degradation of each PRX was analyzed using UV-vis spectroscopy and SEC. UV-vis absorption spectra were obtained using a V-550 UV/vis spectrophotometer (Jasco, Tokyo, Japan).

2.6. Preparation and characterization of PTX-loaded Pr-PD-PRX

A stock solution of PTX (1.25 mL, 2 mg mL^{-1} in DMSO) was combined with the Pr-PD-PRX solution (1.25 mL, 2 mg mL^{-1} in DMSO). Under this condition, the feed loading of PTX was 50 wt%. The solutions were then dialyzed against distilled water using a Spectra/Por 3 (molecular weight cut-off of 3500; Spectrum Laboratories) for 2 days at 4 °C. The recovered solutions were filtered using a 0.45 μm nylon filter to remove undissolved PTX. Small aliquots of the solutions (100 μL) were used to determine the concentration of PTX using high-performance liquid chromatography (HPLC). HPLC was performed using an HPLC system consisting of an AS-950 autosampler (Jasco), a DG-2080-53 degasser (Jasco), a PU-980 pump (Jasco), a CO-965 column oven (Jasco), an RI-2031 Plus RI detector (Jasco), a UV-970 UV-vis detector, and a Cosmosil 5C18-AR-II packed column (250 mm × 4.6 mm internal diameter; Nacalai Tesque, Kyoto, Japan). Sample solutions were injected into the system and were eluted with acetonitrile : distilled water (6 : 4 vol ratio)

Table 1 Characteristics of PRX used in this study

Sample name	Stopper molecule	Number of threading α-CD in PRX	Number of propionyl groups on PRX	M_n
PD-PRX	4,5-Dimethoxy 2-nitrobenzyl	182 (16.1%)	—	278 000
Pr-PD-PRX	4,5-Dimethoxy 2-nitrobenzyl	182 (16.1%)	1197 (6.5/CD)	345 000
ND-PRX	Adamantyl	223 (19.6%)	—	317 000
Pr-ND-PRX	Adamantyl	223 (19.6%)	1552 (6.98/CD)	404 000

at a flow rate of 1.0 mL min^{-1} at 30 °C. Chromatograms were recorded by measuring the absorption at 227 nm, and the concentration of PTX was calculated based on PTX calibration curve. The diameter of the PTX-loaded Pr-PD-PRXs was determined using a Zetasizer Nano ZS (Malvern Instruments, Malvern, UK) equipped with a 4 mW He–Ne laser (633 nm). Dynamic light scattering (DLS) measurements were performed at a detection angle of 173° at 25 °C at 1.0 mg mL^{-1} concentration.

2.7. UV-induced degradation of Pr-PD-PRX nanoparticles

PTX-loaded Pr-PD-PRX solutions were exposed to UV light for 30 min. Subsequently, PTX-loaded Pr-PD-PRX (60 μg PTX) were placed inside a dialysis membrane tube (Spectra/Por 4; molecular weight cut-off of 12 000–14 000). The dialysis process was conducted in 60 mL of phosphate-buffered saline (PBS; 10 mM Na_2HPO_3/NaH_2PO_3, 150 mM NaCl, pH 7.4) containing 0.4% bovine serum albumin (BSA; Fujifilm Wako Pure Chemical) at 37 °C. The outer medium was collected at specific intervals and added fresh medium. PTX was extracted from the outer medium with chloroform, followed by the evaporation of chloroform to dryness under a nitrogen stream. The amount of PTX released was determined using HPLC, as described above.

2.8. Cytotoxicity assay

HeLa cells, derived from human cervical carcinoma, were obtained from the Japanese Collection of Research Bioresources (JCRB, Osaka, Japan). The cells were cultured in Dulbecco's modified Eagle's medium (DMEM; Fujifilm Wako Pure Chemical) supplemented with 10% heat-inactivated fetal bovine serum (FBS; Gibco, Grand Island, NY, USA), 100 units per mL penicillin (Fujifilm Wako Pure Chemical), and 100 μg mL^{-1} streptomycin (Fujifilm Wako Pure Chemical) in 5% CO_2 at 37 °C. Cells were plated in 96-well plates (Thermo Fisher Scientific, Waltham, MA, USA) at a density of 5×10^3 cells per well and incubated overnight. The medium was then changed to a treatment medium containing PTX, PTX-loaded Pr-PD-PRX, or PTX-loaded Pr-ND-PRX. The plates were irradiated with UV light (365 nm) for 30 min and incubated for 48 h. After incubation, 10 μL Cell Counting Kit-8 reagent (Dojindo Laboratories, Kumamoto, Japan) was added to each well and incubated for 1 h at 37 °C. Absorbance was measured at 450 nm using a Varioskan LUX multimode microplate reader (Thermo Fisher Scientific). Cell viability was calculated relative to that of untreated cells.

3. Results and discussion

3.1. Synthesis and characterization of Pr-PD-PRX

PD-PRX, which dissociate under UV irradiation, were synthesized using bulky 4,5-dimethoxy-2-nitrobenzyl groups as photolabile stopper molecules.[17,18] We utilized 4,5-dimethoxy-2-nitrobenzyl 4-nitrophenyl carbonate as a capping agent for preparing PD-PRX (Fig. 2, ESI Fig. S1†). SEC measurements revealed that the peak of PD-PRX was observed at a shorter retention time than that of axial PEG-NH_2 (Fig. 3a). Additionally, the peak of PD-PRX was observed in a UV-detected SEC chart, whereas α-CD and PEG-NH_2 showed no peaks. Because the 4,5-dimethoxy-2-nitrobenzyl moieties absorb light with a wavelength of 350–360 nm,[17,18] PD-PRX showed a peak in UV detection. Additionally, peaks corresponding to the 4,5-dimethoxy-2-nitrobenzyl groups were observed at 7.01 and 7.69 ppm in the ^1H NMR spectrum of PD-PRX (Fig. 3b). These results suggested that PD-PRX capped with bulky 4,5-dimethoxy-2-nitrobenzyl groups as stopper molecules were successfully synthesized. From the ^1H NMR spectrum, the number of threading α-CD in PD-PRX was determined to be 182, corresponding to a 16.1% threading ratio, assuming one α-CD molecule includes two repeating ethylene glycol units.[32] As

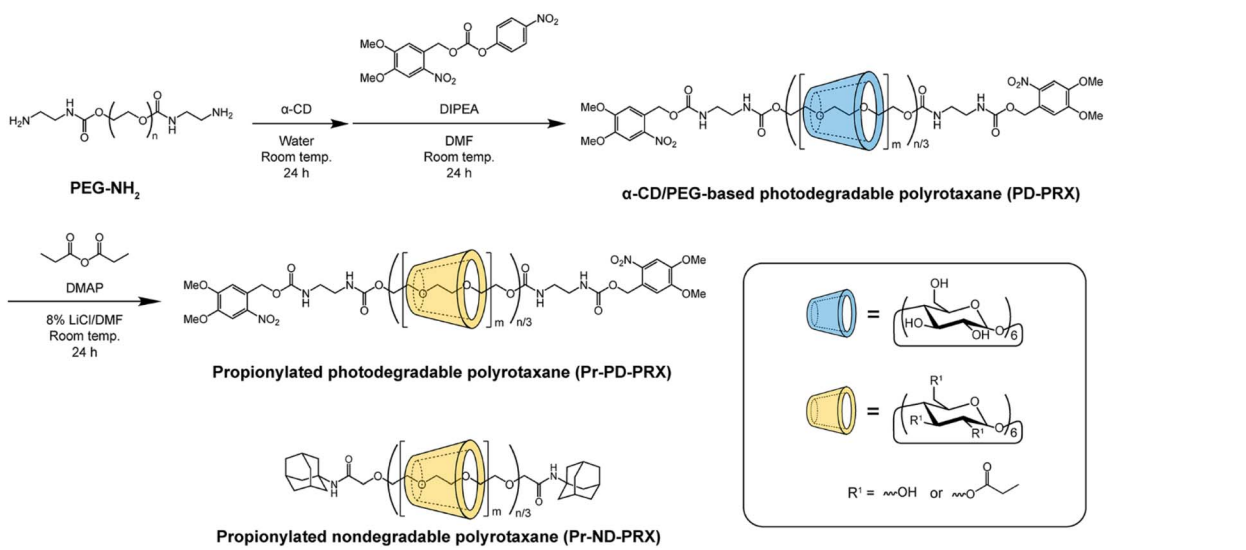

Fig. 2 Synthesis scheme for propionylated α-CD/PEG-based photodegradable PRX capped with 4,5-dimethoxy-2-nitrobenzyl groups (Pr-PD-PRX) and the chemical structure of propionylated nondegradable PRX (Pr-ND-PRX). *n* and *m* denote the degree of polymerization of PEG and the number of threading α-CD, respectively.

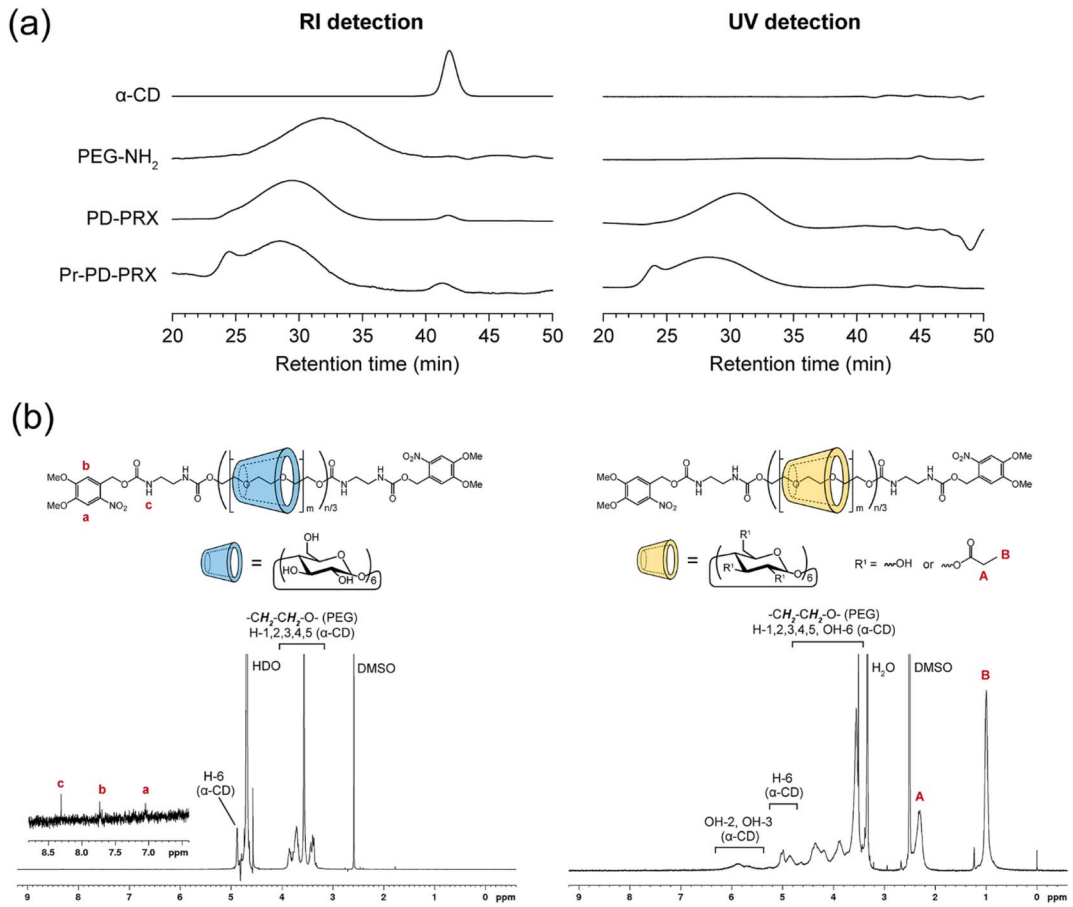

Fig. 3 (a) SEC charts of α-CD, PEG-NH_2, PD-PRX, and Pr-PD-PRX eluted with DMSO containing 10 mM LiBr at 60 °C. The peaks were detected in refractive index (RI) and UV absorption at 352 nm. (b) ^{1}H NMR spectra of PD-PRX in NaOD/D_2O at 25 °C and Pr-PD-PRX in DMSO-d_6 at 25 °C.

a control, ND-PRX capped with adamantyl groups was synthesized and characterized similarly (Fig. S2 and S3†).

Next, we modified propionyl groups on the hydroxy groups of threading α-CDs in PD-PRX and ND-PRX, because propionylated PRX can incorporate many drugs with good stability.[22] The modification of propionyl groups on the hydroxy groups of threading α-CDs was performed according to the previous study,[22] and the resulting PRXs were analyzed with SEC, ^{1}H NMR, and Fourier-transform infrared (FT-IR) spectra. SEC results confirmed that PRX degradation did not occur during the reaction or purification processes (Fig. 3a). However, a new peak was observed at 24.5 min, presumably due to the aggregation of PD-PRX. ^{1}H NMR spectrum confirms that new peaks assigned to propionyl groups are clearly marked at 1.00 and 2.31 ppm, indicating that the propionyl groups were modified on PD-PRX (Fig. 3b). Additionally, in the FT-IR spectrum of Pr-PD-PRX, new peaks corresponding to ester linkages were observed at 1280 and 1743 cm^{-1} (ESI Fig. S4†). These data confirmed the successful synthesis of Pr-PD-PRX. Based on the ^{1}H NMR results, the number of modified propionyl groups in Pr-PD-PRX was 1197 (Table 1). Propionyl group-modified ND-PRX (Pr-ND-PRX) was synthesized and characterized similarly (ESI Fig. S2–S4†). The number of modified propionyl groups was 1552, based on the ^{1}H NMR spectrum of Pr-ND-PRX (Table 1, ESI Fig. S2†).

3.2. UV-induced dissociation of Pr-PD-PRX

To verify the photodegradability of Pr-PD-PRX, we measured the changes in the UV-vis absorption spectra of Pr-PD-PRX after UV irradiation (Fig. 4). Before UV irradiation, Pr-PD-PRX showed a maximum absorption at 360 nm derived from the terminal 4,5-dimethoxy 2-nitrobenzyl groups. After irradiation with UV light (365 nm), the peak intensities gradually decreased with increasing irradiation time. This spectral change suggests that the degradation of the 4,5-dimethoxy 2-nitrobenzyl groups occurred upon UV irradiation.

To assess whether Pr-PD-PRX dissociated upon UV irradiation, SEC measurements were performed. After UV irradiation for 1 min, the peak corresponding to dethreaded α-CDs was observed at 41.2 min in RI-detected SEC charts (Fig. 5a). Additionally, several new peaks derived from liberated 4,5-dimethoxy 2-nitrobenzyl groups and their byproducts were observed at 44.1, 44.8, and 46.7 min in UV-detected SEC charts (Fig. 5a). With increasing the irradiation time, the peak intensity of Pr-PD-PRX decreased, whereas the peak intensities of dethreaded propionylated α-CD (Pr-α-CD) and 4,5-dimethoxy 2-nitrobenzyl groups increased. After 30 min of UV irradiation, most parts of Pr-PD-PRX were dissociated, and only the peak of dethreaded Pr-α-CD was detected. In contrast, the SEC chart of Pr-ND-PRX

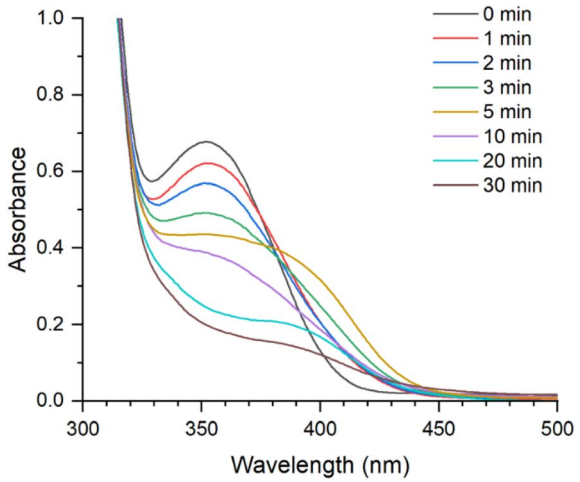

Fig. 4 UV-vis absorption spectra of Pr-PD-PRXs after UV light (365 nm) irradiation for 0 to 30 min in DMSO (5 mg mL^{-1}) at 25 °C.

remained unchanged even after 30 min of UV irradiation (Fig. 5b), suggesting that Pr-ND-PRX was intrinsically stable against UV light. In the case of our previously reported photodegradable PRXs capped with *o*-nitrobenzyl or trithiocarbonate groups, it was difficult to completely dissociate PRXs by UV irradiation.[14–16] Therefore, Pr-PD-PRX exhibited superior photodegradability compared to the previously reported photodegradable PRXs.[14–16]

3.3. Photodegradation of PTX-loaded Pr-PD-PRX and UV-induced drug release

Acylated PRXs comprising high-molecular-weight PEG axles can form self-assembled nanoparticles in aqueous solutions and encapsulate hydrophobic drugs through the hydrophobic interactions of acyl groups.[21,22] However, the release rate of drugs needs to be improved because the release rate is less than 60%. We hypothesized that the UV-induced dissociation of Pr-PD-PRX improves the drug release rate. Self-assembled nanoparticles of Pr-PD-PRX and Pr-ND-PRX loaded with hydrophobic PTX were prepared using the dialysis method.[21,22] The loading contents of PTX in Pr-PD-PRX and Pr-ND-PRX were determined to be 12.7 and 13.6 wt%, respectively, by HPLC measurements. DLS measurements revealed that the PTX-loaded Pr-PD-PRX showed unimodal distribution with 150.0 ± 3.8 nm in diameter (Fig. 6a), which was close to the diameter of empty Pr-PD-PRX nanoparticles (159.1 ± 17.5 nm). Similarly, the diameters of the empty and PTX-loaded Pr-ND-PRX nanoparticles were determined to be 187.4 ± 4.0 nm and 171.1 ± 0.3 nm, respectively (Fig. 6b). The diameters of the nanoparticles were roughly identical, regardless of the PTX loading and the structure of the stopper molecules.

Next, the UV-induced collapse of PTX-loaded nanoparticles was assessed by measuring scattering light intensity because the scattered light intensity of nanoparticles depended on the sixth power of the diameter in Rayleigh scattering.[33] After 30 min of UV irradiation, the scattering light intensity of PTX-loaded Pr-PD-PRX nanoparticles decreased to 3.3% (Fig. 6c). In contrast, the scattered light intensities of the PTX-loaded Pr-ND-PRX nanoparticles remained unchanged after UV irradiation. This result strongly suggests that the PTX-loaded Pr-PD-PRX nanoparticles collapsed because the UV-induced dissociation of Pr-PD-PRX.

The release profiles of PTX from the Pr-PD-PRX and Pr-ND-PRX nanoparticles are shown in Fig. 7. Without UV light irradiation, the release profiles of PTX from the Pr-PD-PRX and Pr-ND-PRX nanoparticles seemed to be approximated by two-phase zero-order kinetics. PTX was linearly released from the nanoparticles at initial stage (0 to 14 h). This rapid release process is owing to the release of PTX which is loosely associated into the self-assembled nanoparticles. After the release of loosely associated PTX, stably encapsulated PTX was remained into the nanoparticles. Subsequently, the stably encapsulated PTX was slowly released from the nanoparticles. Therefore, the drug release from the Pr-PD-PRX and Pr-ND-PRX nanoparticles occurred in two phases. At 24 h, the release rates of PTX from Pr-PD-PRX and Pr-ND-PRX nanoparticles were almost identical

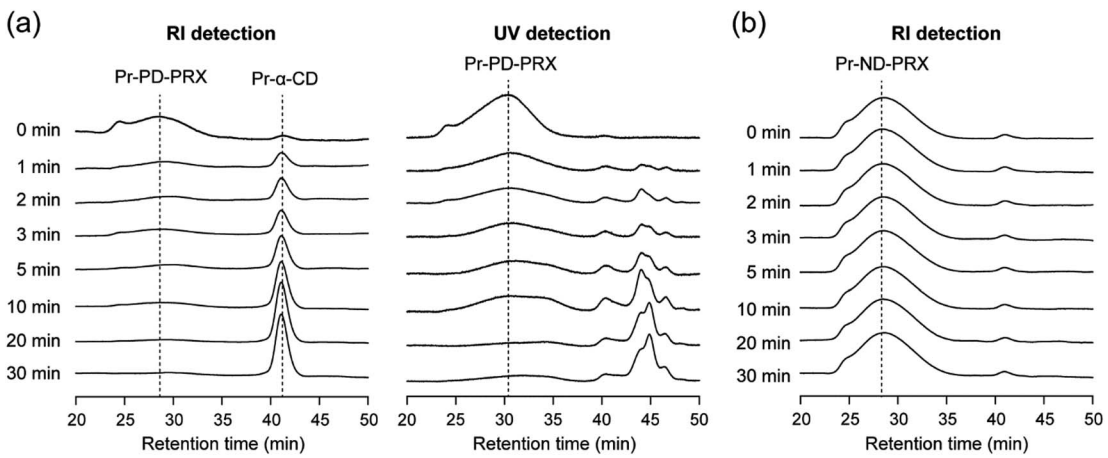

Fig. 5 SEC charts of Pr-PD-PRX and Pr-ND-PRX eluted with DMSO containing 10 mM LiBr at 60 °C after UV irradiation for 0 to 30 min. (a) RI and UV (352 nm) detections for Pr-PD-PRX and (b) RI detection for Pr-ND-PRX.

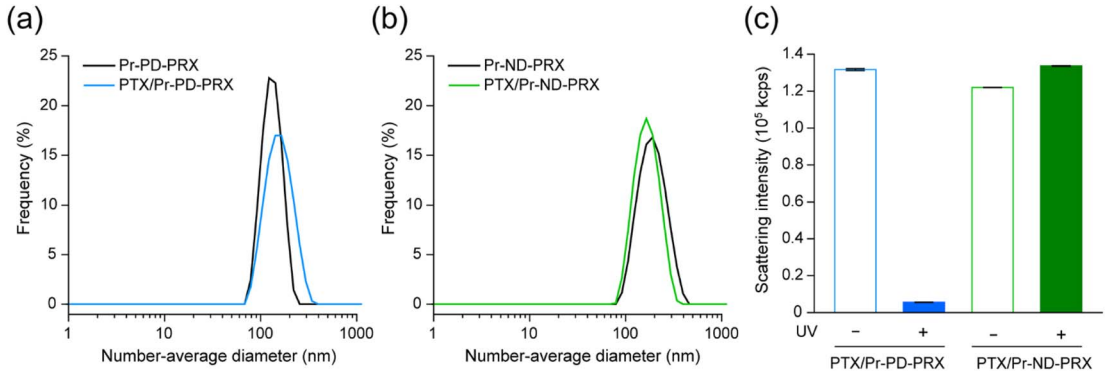

Fig. 6 (a) Distributions of the number-average diameter of Pr-PD-PRX and PTX-loaded Pr-PD-PRX in distilled water (0.5 mg mL^{-1}). (b) Distributions of the number-average diameter of Pr-ND-PRX and PTX-loaded Pr-ND-PRX in distilled water (0.5 mg mL^{-1}). (c) Scattering intensities of PTX-loaded Pr-PD-PRX and Pr-ND-PRX before and after UV irradiation (365 nm) for 30 min. Data are expressed as mean ± standard deviation (SD, $n = 3$).

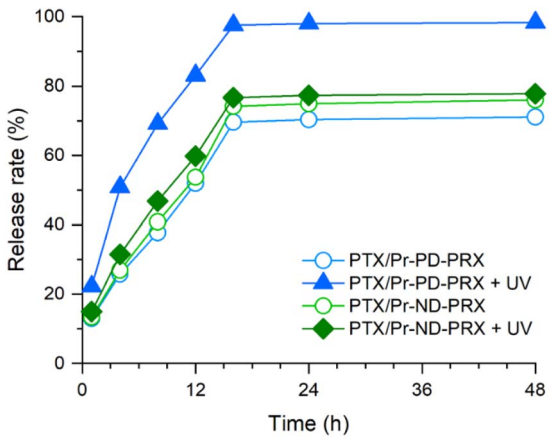

Fig. 7 Time courses of the cumulative PTX release from PTX/Pr-PD-PRX (open blue circles), PTX/Pr-ND-PRX (open green circles), PTX/Pr-PD-PRX after UV irradiation for 30 min (closed triangles), and PTX/Pr-ND-PRX after UV irradiation for 30 min (closed diamonds) in PBS at 37 °C.

(70.3–77.4%) without UV irradiation. However, when the release profiles were assessed after 30 min of UV irradiation, the release of PTX was accelerated and completely released from the Pr-PD-PRX nanoparticles after 14 h. In contrast, the release of PTX did not accelerate for Pr-ND-PRX after UV irradiation. To date, photodegradable drug carriers such as the self-assembled polymeric micelles were reported.[34] For example, the block copolymers containing photolabile coumarin moieties in the side chain were developed to prepare photodegradable polymeric micelles and photo-triggered release of PTX. However, the loaded PTX was not completely released from the polymeric micelles. Because the cleavage of multiple photolabile moieties is required for the collapse of the polymeric micelles, the release rate of PTX is limited. On the other hand, the Pr-PD-PRXs are dissociated by the cleavage of only one site of 4,5-dimethoxy 2-nitrobenzyl stoppers. Therefore, UV-induced collapse of Pr-PD-PRX nanoparticles occurs efficiently compared to previous photodegradable polymeric micelles, leading to the complete release of PTX by UV irradiation.

3.4. Cytotoxicity PTX-loaded Pr-PD-PRX

To clarify the contribution of the UV-induced release of PTX in the drug delivery system (DDS), we tested the cytotoxicity of PTX-loaded Pr-PD-PRX nanoparticles in HeLa cells. After the PTX-loaded Pr-PD-PRX nanoparticles were added in the culture medium, the cells were irradiated with UV light for 30 min, followed by incubation for 48 h. In our previous study, the viability of the cells treated with PTX decreased after 48 h of treatment.[22] Therefore, we tested the viability of cells after 48 h of treatment. The IC_{50} values for free PTX and PTX-loaded Pr-PD-PRX were determined to be 13.6 and 53.9 ng mL^{-1}, respectively (Fig. 8). Consistent with previous reports, PTX-loaded acylated PRX nanoparticles showed lower cytotoxicity than free PTX, most likely because of the limited release of PTX.[21,22] However, under UV irradiation, the cytotoxicity of PTX-loaded Pr-PD-PRX was similar to that of free PTX (Fig. 8a), and the IC_{50} value was determined to be 16.8 ng mL^{-1}. In contrast, the cytotoxicity of PTX-loaded Pr-ND-PRX was not affected by UV irradiation (Fig. 8b). The IC_{50} values for PTX-loaded Pr-ND-PRX without UV irradiation was 38.0 ng mL^{-1}, whereas the IC_{50} values for PTX-loaded Pr-ND-PRX after UV irradiation was 45.1 ng mL^{-1}. These results suggested that the UV-induced release of PTX from Pr-PD-PRX nanoparticles enhance cytotoxicity. Our group has developed anticancer drug-conjugated acid-degradable PRXs to promote the intracellular release of anticancer drugs.[35] However, the cytotoxicity of drug-conjugated PRX is lower than that of free drugs, presumably because the number of modified drugs on PRX is limited. In contrast, photodegradable Pr-PD-PRX can encapsulate large amount of hydrophobic drugs in the hydrophobic domain and release all drugs upon UV irradiation. We conclude that photodegradable Pr-PD-PRX is a rational molecular design of photoresponsive polymeric drug carriers for efficiently collapsing self-assembled nanoparticles and releasing loaded drugs by UV irradiation. However, UV light has limited penetration into deep site of

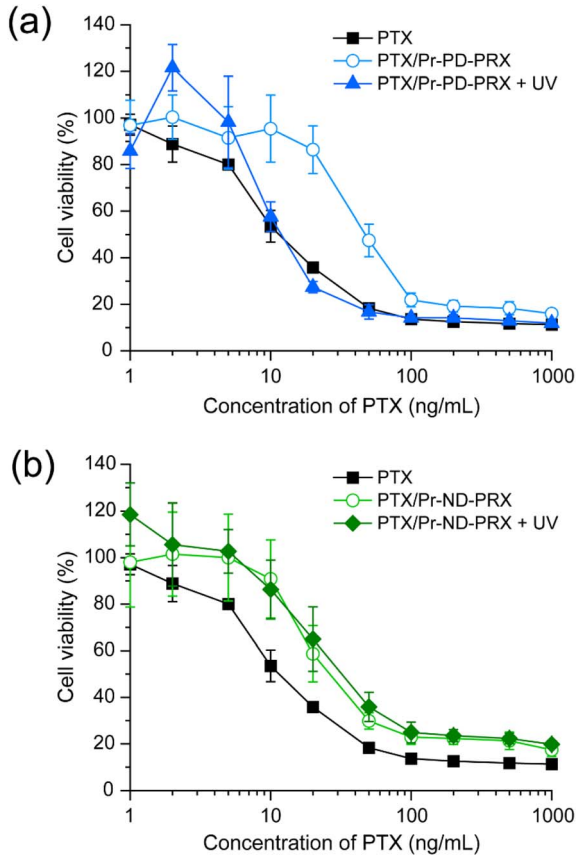

Fig. 8 (a) Viability of HeLa cells treated with PTX (squares), PTX/Pr-PD-PRX (open circles), and PTX/Pr-PD-PRX with UV irradiation (closed triangles) for 48 h. (b) Viability of HeLa cells treated with PTX (squares), PTX/Pr-ND-PRX (open circles), and PTX/Pr-ND-PRX with UV irradiation (closed diamonds) for 48 h. The viability of untreated and non-irradiated cells was adjusted at 100%. Data are expressed as mean ± SD ($n = 6$).

biological tissues and may damage the periphery of biological tissues. This system should be improved using near-infrared cleavable stopper molecules or two-photon excitation systems.[36,37]

4. Conclusion

In the present study, we developed photodegradable polyrotaxanes comprising propionylated α-CD as a cyclic host, high molecular weight PEG as a polymer axis, and 4,5-dimethoxy 2-nitrobenzyl groups as a UV-cleavable bulky stopper molecules for facilitating UV-induced drug release from acylated PRX nanoparticles. Pr-PD-PRX was completely dissociated into constituent PEG and α-CD by UV irradiation (365 nm) for 30 min. Additionally, Pr-PD-PRX formed self-assembled nanoparticles in an aqueous solution, which enabled the encapsulation of hydrophobic PTX in its hydrophobic domain. These Pr-PD-PRX nanoparticles were degraded by UV irradiation, which promoted the release of encapsulated PTX compared to nondegradable Pr-ND-PRX nanoparticles. Moreover, UV irradiation of PTX-loaded Pr-PD-PRX nanoparticles resulted in higher cytotoxicity than that of non-irradiated Pr-PD-PRX and nondegradable Pr-ND-PRX through the enhanced intracellular release of encapsulated PTX. The findings of this study provide new insights into the development of intelligent DDS functional nanomaterials using supramolecular polymers.

Conflicts of interest

There are no conflicts to declare.

Acknowledgements

This study was financially supported by Japan Society for the Promotion of Science (JSPS) KAKENHI (JP20H04527) and TMDU wise program.

References

1 G. Wenz, B.-H. Han and A. Müller, *Chem. Rev.*, 2006, **106**, 782.
2 A. Harada, A. Hashidzume, H. Yamaguchi and Y. Takashima, *Chem. Rev.*, 2009, **109**, 5974.
3 A. Harada, J. Li and M. Kamachi, *Nature*, 1992, **356**, 325.
4 J. Li and X. J. Loh, *Adv. Drug Delivery Rev.*, 2008, **60**, 1000.
5 S. Loethen, J. M. Kim and D. H. Thompson, *Polym. Rev.*, 2007, **47**, 383.
6 A. Tamura and N. Yui, *Chem. Commun.*, 2014, **50**, 13433.
7 T. Higashi, D. Iohara, K. Motoyama and H. Arima, *Chem. Pharm. Bull.*, 2018, **66**, 207.
8 Z. Liu, L. Ye, J. Xi, J. Wang and Z.-G. Feng, *Prog. Polym. Sci.*, 2021, **118**, 101408.
9 N. Yui and T. Ooya, *Chem.–Eur. J.*, 2006, **12**, 6730.
10 A. Tamura, Y. Arisaka and N. Yui, *Kobunshi Ronbunshu*, 2017, **74**, 239.
11 T. Ooya, H. S. Choi, A. Yamashita, N. Yui, Y. Sugaya, A. Kano, A. Maruyama, H. Akita, R. Ito, K. Kogure and H. Harashima, *J. Am. Chem. Soc.*, 2006, **128**, 3852.
12 A. Tamura and N. Yui, *J. Controlled Release*, 2018, **269**, 148.
13 Z. Liu, G. A. Simchick, J. Qiao, M. M. Ashcraft, S. Cui, T. Nagy, Q. Zhao and M. P. Xiong, *ACS Nano*, 2021, **15**, 419.
14 J.-H. Seo, M. Fushimi, N. Matsui, T. Takagaki, J. Tagami and N. Yui, *ACS Macro Lett.*, 2015, **4**, 1154.
15 S. Matsunaga, A. Tamura, M. Fushimi, H. Santa, Y. Arisaka, T. Nikaido, J. Tagami and N. Yui, *ACS Appl. Polym. Mater.*, 2020, **2**, 5756.
16 T. W. Kang, A. Tamura, Y. Arisaka and N. Yui, *Polym. Chem.*, 2021, **12**, 3794.
17 A. Qian, K. Liu, P. Chen, Y. Yao, J. Yan, W. Li, X. Zhang and A. Zhang, *Macromolecules*, 2019, **52**, 3454.
18 S. Zheng, K. Liu, P. Chen, C. Song, J. Yan and A. Zhang, *Macromolecules*, 2022, **55**, 7127.
19 S. Hayakawa, A. Tamura, N. Nikiforov, H. Koike, F. Kudo, Y. Cheng, T. Miyazaki, M. Kubekina, T. V Kirichenko, A. N. Orekhov, N. Yui, I. Manabe and Y. Oishi, *JCI Insight*, 2022, **7**, e138539.
20 W. K. Lee, T. Ichi, T. Ooya, T. Yamamoto, M. Katoh and N. Yui, *J. Biomed. Mater. Res., Part A*, 2003, **67A**, 1087.

21 A. Tonegawa, A. Tamura and N. Yui, *ACS Macro Lett.*, 2019, **8**, 826.
22 A. Tonegawa, A. Tamura, S. Zhang and N. Yui, *Polymer*, 2020, **200**, 122537.
23 A. Tonegawa, A. Tamura and N. Yui, *Macromol. Rapid Commun.*, 2020, **41**, 2000322.
24 A. Tamura, M. Ohashi, A. Tonegawa, T. W. Kang, S. Zhang and N. Yui, *Macromol. Chem. Phys.*, 2021, **222**, 2000420.
25 A. Tamura, T. W. Kang, A. Tonegawa, Y. Arisaka, H. Masuda, R. Mikami, T. Iwata, T. Yoda and N. Yui, *Biomacromolecules*, 2022, **23**, 4860.
26 O. Bertranda and J.-F. Gohy, *Polym. Chem.*, 2017, **8**, 52.
27 H. Zhao, E. S. Sterner, E. B. Coughlin and P. Theato, *Macromolecules*, 2012, **45**, 1723.
28 B. Zheng, L. Yu, H. Dong, J. Zhu, L. Yang and X. Yuan, *Polymers*, 2022, **14**, 2416.
29 N. Doi, Y. Yamauchi, R. Ikegami, M. Kuzuya, Y. Sasai and S. Kondo, *Polym. J.*, 2020, **52**, 1375.
30 W. Hou, R. Liu, S. Bi, Q. He, H. Wang and J. Gu, *Molecules*, 2020, **25**, 5147.
31 A. Tamura and N. Yui, *Biomaterials*, 2013, **34**, 2480.
32 A. Harada, J. Li and M. Kamachi, *Macromolecules*, 1993, **26**, 5698.
33 R. M. Metzger, in *The Physical Chemist's Toolbox*, ed. R. M. Metzger, John Wiley & Sons, Hoboken, New Jersy, USA, 2012, ch. 3.
34 S. Kumar, J.-F. Allard, D. Morris, Y. L. Dory, M. Lepage and Y. Zhao, *J. Mater. Chem.*, 2012, **22**, 7252.
35 A. Tamura, M. Osawa and N. Yui, *Molecules*, 2023, **28**, 2517.
36 B. Sana, A. Finne-Wistrand and D. Pappalardo, *Mater. Today Chem.*, 2022, **25**, 100963.
37 X. Zeng, X. Zhou and S. Wu, *Macromol. Rapid Commun.*, 2018, **39**, 1800034.